Vitamin D Receptor Upregulates Tight Junction Protein Claudin-5 against Tumorigenesis

Yongguo Zhang [1], Shari Garrett[1], Robert E. Carroll[1], Yinglin Xia[1], and Jun Sun [2,3,4] *

1. Department of Medicine, College of Medicine, University of Illinois at Chicago, Chicago, IL, USA

2. UIC Cancer Center, University of Illinois at Chicago, Chicago, IL, USA

3. Department of Microbiology/Immunology, College of Medicine, University of Illinois at Chicago, Chicago, IL, USA

4. Jesse Brown VA Medical Center Chicago, IL (537), USA

Correspondence:

Jun Sun, Ph.D., Professor, AGAF, FAPS

junsun7@uic.edu

Author Contributions: YZ: acquisition, analysis, and interpretation of data, drafting of the manuscript, and statistical analysis, SG: assistance with western blots and TJ data. YX: Statistical analysis, microbiome data analysis, and manuscript drafting. REC: Provided human biopsies and clinical perspectives of CRC. JS: study concept and design, analysis and interpretation of data, writing of the manuscript for important intellectual content, obtaining funding, and study supervision.

Funding: This research was funded by the UIC Cancer Center, the NIDDK/National Institutes of Health grants R01DK105118 and R01DK114126, VA Merit Award 1 I01 BX004824-01, and DOD BC160450P1 to Jun Sun**.** The study sponsors played no role in the study design, data collection, analysis, and interpretation of data.

Acknowledgments: We would like to thank Dr. David Zhou for assisting with the CRC human samples, Drs. Shaoping Wu and Rong Lu for assisting with the AOM/DSS model, and Jason S. Xia for proofreading. The contents do not represent the views of the United States Department of Veterans Affairs or the United States Government.

Conflicts of Interest: The authors declare no conflict of interest. The funders played no role in the study design, the collection, analyses, or interpretation of data, the writing of the manuscript, or the decision to publish the results.

A short summary

1. What is already known about this subject?

- Tight junction structures are essential for intestinal barrier integrity, inflammation, and cancer.
- Vitamin D deficiency and the vitamin D receptor (VDR) play important roles in the development of colon cancer.

2. What are the new findings?

- Our study is the first to link barrier function, a specific tight junction protein, and genetic susceptibility through intestinal epithelial VDR in human colorectal cancer.
- Our study fills an existing gap by characterizing the mechanism of intestinal epithelial VDR in regulating barrier functions through alterations in TJs in tumorigenesis. VDR is important for the maintenance of the physiological level of the TJ protein Claudin-5 in the colon. The *CLDN-5* gene is a downstream target of the VDR signaling pathway. Lack of VDR led to a reduction of Claudin-5 in tumors, whereas enhancing VDR increased Claudin-5 to protect the intestinal epithelial cells from tumorigenesis.
- We report fecal VDR reduction in a colon cancer model. This introduces the possibility for the identification of new biomarkers and therapeutic targets to restore VDR-dependent functions in CRC.

3. How might it impact on clinical practice in the foreseeable future

- Diagnosis of CRC considering VDR status
- Barrier: direct, indirect biomarkers
- Intestinal barriers in cancer prevention and treatment

58 Barrier function and VDR are not only essential for the maintenance of intestinal
59 homeostasis, but they are also critical for the development of chronic mucosal inflammation
60 and cancer. This knowledge can be immediately used to develop intestinal VDR and
61 Claudin-5 as clinical biomarkers for identifying patients who may benefit from currently
62 available interventions and could also be used for the eventual development of novel
63 strategies for the prevention and treatment of human CRC.
64

Abstract:

Background/Objective: Tight junctions (TJs) are essential for barrier integrity, inflammation, and cancer. The TJ protein Claudin-5 in the epithelia forms paracellular barriers and pores for permeability. Vitamin D and the vitamin D receptor (VDR) play important roles in various cancers. Although VDR and Claudin-5 are all involved in colorectal cancer (CRC), it remains unclear if they are closely related or function independently. **Design:** Using the human CRC database, we explored the correlation between VDR and Claudin-5. We then investigated the VDR regulation of Claudin-5 using VDR knockout ($VDR^{-/-}$) and intestinal epithelial VDR knockout mice ($VDR^{\Delta IEC}$) with chemical-induced colon cancer and an epithelial VDR overexpression model. Human samples, organoids, and intestinal epithelial cells were used to determine the underlying mechanisms. **Results:** In human colon cancer, colonic VDR expression was low and was significantly correlated with a reduction of Claudin-5 mRNA and protein. In the colon of $VDR^{-/-}$ and $VDR^{\Delta IEC}$ mice, deletion of VDR led to lower protein and mRNA levels of Claudin-5. Intestine permeability was increased in the AOM-DSS-induced $VDR^{-/-}$ colon cancer model. Lack of VDR and a reduction of Claudin-5 are associated with an increased number of tumors in the $VDR^{-/-}$ and $VDR^{\Delta IEC}$ mice. Furthermore, gain and loss of function studies have identified *CLDN-5* as a downstream target of the VDR signaling pathway. Epithelial VDR overexpression protected against the loss of Claudin 5 in response to intestinal inflammation **Conclusion:** This study advances the understanding of how VDR regulates intestinal barrier functions in tumorigenesis as a biomarker and potential treatment.

87

88 **Keywords:** Claudin, barrier function, inflammation, colon cancer, colitis, tight junction,

89 Vitamin D, vitamin D receptor

90

Introduction

Tight junction structures are essential for intestinal innate immunity and barrier function. The disruption of TJs is a common manifestation of various diseases, including chronic inflammation and cancer. Changes in the expression and distribution of TJ proteins such as Claudin-2, -5, and -8 lead to discontinuous TJs and barrier dysfunction in active Crohn's disease (CD), a type of inflammatory bowel disease [1]. Claudin-5 is expressed in the epithelia and endothelia and forms paracellular barriers and pores that determine permeability. This protein is downregulated in colon cancer [2, 3].

VDR is a nuclear receptor that mediates most known functions of the biologically active form of vitamin D [4, 5, 6]. VDR possesses multiple critical functions in regulating innate and adaptive immunity, intestinal homeostasis, host response to microbiota, and tight junction structure [7, 8, 9, 10, 11, 12, 13, 14]. Vitamin D/VDR deficiency has been implicated in patients with inflammatory bowel disease and colon cancer [15, 16, 17, 18, 19, 20, 21]. Our study demonstrated that VDR is essential for maintaining intestinal and microbial homeostasis [22] and for protecting against intestinal tumorigenesis [23] [24]. Although vitamin D has been extensively studied, many critical questions regarding the biological functions of intestinal VDR in CRC remain unanswered. Although VDR and TJ proteins (e.g., Claudins) are involved in colon cancer, it remains unclear if they are closely related or function independently. Considering the multiple functional roles of VDR in the development of colon cancer [20, 24], it is important to dissect the cellular and molecular

112 mechanisms by which VDR contributes to barrier function in protecting the host from
113 tumorigenesis.
114
115 Here, we revisited the human CRC database and determined that colonic VDR expression
116 is low and positively correlated with the reduction of the TJ protein Claudin-5 in CRC,
117 including colitis-associated colon cancer. We investigated the novel role of VDR in
118 regulating Claudin-5 expression using $VDR^{-/-}$ and intestinal epithelial VDR knockout mice
119 ($VDR^{\Delta IEC}$) in a colitis-associated colon cancer model. Human organoids, human colon
120 cancer samples, $VDR^{-/-}$ mouse embryonic fibroblasts (MEF) cells, and cultured intestinal
121 epithelial cells were used to determine the molecular mechanisms. We determined that
122 VDR is an important transcriptional regulator for the maintenance of physiological levels of
123 the target gene *Claudin-5* in the intestine. Furthermore, we generated a conditional
124 intestinal epithelial VDR-overexpressed mouse model to study the protective role of VDR in
125 the maintenance of TJs in the context of inflammation. Our goal was to provide a detailed
126 understanding of how VDR status contributes to intestinal inflammation and cancer. Our
127 findings may offer an additional avenue to treat colon cancer by restoring barrier functions
128 and developing a new protocol for risk assessment and prevention of cancer.
129
130

Results

Reduced VDR was positively correlated with low Claudin-5 expression in CRC patients

We first examined the gene expression levels of VDR and Claudin-5 in normal and human CRC samples by reviewing the GEO databases GSE 4183 and GSE 8671 from Affymetrix data (human genome U133 Plus 2.0 arrays). Reduced VDR and Claudin-5 expression was observed in patients with CRC (**Fig. 1A**). To quantify and visualize the correlations between intestinal Claudin-5 and the VDR protein, we performed a regression analysis of VDR against Claudin-5 and conducted a scatter plot with a regression line (**Fig. 1B**). We found significantly coordinated expression of VDR and Claudin-5 in biopsy samples collected from patients with CRC. We further analyzed data obtained from human colitis-associated colon cancer (**Fig. 1C)**. VDR and Claudin-5 expression was significantly reduced in patients with colitis-associated CRC (GEO database GSE8671, GSE10714, and GSE37283) (**Fig. 1C)**. We identified a positive correlation between VDR and Claudin-5 in biopsy samples collected from colitis-associated CRC patients and healthy controls (**Fig. 1D)**. We then examined the protein levels of intestinal VDR in normal and CRC human colon samples using IHC. Compared to normal intestines, CRC patients with CRC possessed significantly lower VDR expression (**Fig. 1E)**. Immunofluorescence (IF) staining of Claudin-5 revealed significantly lower Claudin-5 expression in CRC human colon samples (**Fig. 1F)**. We performed correlation analysis and scatter plots of the staining intensity changes between the VDR protein and Claudin-5 in the colon. The results revealed that the staining intensity of Claudin-5 and intestinal VDR was positively associated with the Pearson correlation

coefficient **(Fig. 1G)**. Thus, we revealed that colonic VDR expression is low and is correlated with the reduction of Claudin-5 at both mRNA and protein levels in human CRC, including colitis-associated colon cancer.

Larger and more tumors developed in VDR deficient mice

Animal models have been developed to reflect the initiation and progression of human colon cancer [25]. Azoxymethane (AOM) [26] mice develop hyperproliferative colonic mucosa, aberrant crypt foci (ACF), and eventually carcinomas [27]. An AOM–dextran sulfate sodium (DSS) model is widely used to study colitis-associated colon cancer [28]. We next investigated the role of VDR in regulating Claudin-5 expression in the development of cancer using an AOM/DSS-treated mouse model (**Fig. 2A**). For wild-type $VDR^{+/+}$ and whole-body VDR knockout ($VDR^{-/-}$) mice, representative colons with tumors are shown (**Fig. 2B).** We observed that AOM/DSS-treated $VDR^{-/-}$ mice developed more tumors in the colon (**Fig. 2C**). The maximum tumor size was significantly larger in $VDR^{-/-}$ mice compared to that in $VDR^{+/+}$ mice (**Fig. 2D**). Furthermore, pathological analysis of colon samples indicated differences in tumor stage (carcinoma versus adenoma) between $VDR^{-/-}$ mice and the $VDR^{+/+}$ AOM/DSS experimental groups (**Fig. 2E**). Epithelial hyperproliferation plays a critical role in the development of cancer. The IF data of the proliferative marker PCNA revealed that PCNA in the colon was significantly increased in the $VDR^{-/-}$ mice compared to that in the $VDR^{+/+}$ mice (**Fig. 2F**). Chronic inflammation is one of the factors that contribute to CRC. We determined that the serum cytokines TNF-α, IL-1β, and IL-17 were significantly higher in the $VDR^{-/-}$ mice, compared to levels in the $VDR^{+/+}$ mice (**Fig. 2G**).

175

176 **VDR deletion leads to decreased Claudin-5 expression in tumor tissues**

177 We examined changes in barrier function by testing intestinal permeability in mice with or
178 without tumors. Mice were gavaged with fluorescein dextran (molecular weight 3 kDa). After
179 4-h, blood samples were collected for fluorescence intensity measurements. Higher
180 fluorescence intensity is indicative of higher intestinal permeability. As shown in **Fig. 3A**,
181 AOM/DSS treatment induced increased intestinal permeability in both $VDR^{+/+}$ and
182 $VDR^{-/-}$ mice, while the $VDR^{-/-}$ mice exhibited significantly higher permeability
183 post-treatment. Based on the *in vivo* intestinal permeability data, we hypothesized that the
184 TJ proteins would be altered in the AOM/DSS mice. In the $VDR^{-/-}$ mice, we observed
185 significant downregulation of Claudin-5 at the mRNA and protein levels in the colon (**Fig.**
186 **3B & 3C**). Claudin-5 staining was observed at the crypt surface and at the lower portion of
187 the intestine. Reduced Claudin-5 expression was confirmed through the immunostaining of
188 AOM/DSS mice (**Fig. 3D &3G**). However, VDR deletion did not alter the expression of the
189 TJ protein Claudin-7 in the colon of $VDR^{-/-}$ mice compared to that in $VDR^{+/+}$ mice (**Fig. 3E**).
190 VDR expression was also decreased in mice with AOM/DSS-induced colon cancer (**Fig. 3F**
191 **and 3H**). Moreover, we used our recently established method to measure VDR levels
192 according to qPCR in fecal samples [29]. We detected a significant reduction in VDR in
193 fecal samples from mice with tumors (**Fig. 3I**). These data also suggest a decreased VDR
194 in epithelial cells that are shed from mice with tumors.

195

196 **Conditional deletion of intestinal epithelial VDR led to increased permeability and**
197 **reduced Claudin-5 in the AOM/DSS cancer model.**

198 Intestine permeability was also significantly increased in $VDR^{\Delta IEC}$ mice with conditional
199 deletion of intestinal epithelial VDR (**Fig. 4A**). Intestinal epithelial VDR-specific deletion led
200 to significantly decreased Claudin-5 at the mRNA level in the colon (**Fig. 4B**) and further
201 decreased in the mice with colon cancer; however, other Claudin, such as Claudin-7, was
202 not altered in the absence of VDR. At the protein level, we found the reduced Claudin-5 in
203 the $VDR^{\Delta IEC}$ mice (**Fig. 4C**). In tumor tissues of $VDR^{\Delta IEC}$ mice epithelial Claudin-5 was
204 disorganized (**Fig. 4D)** and significantly decreased, compared to that in tumors of VDR^{loxp}
205 mice (**Fig. 4F**). In contrast, Claudin-7 was not altered in tumors from $VDR^{\Delta IEC}$ mice
206 compared to the tumor tissue of VDR^{loxp} mice (**Fig. 4E**). The VDR expression in fecal
207 samples was downregulated in the AOM-DSS VDR^{loxp} mice (**Fig. 4G**).
208
209 **Identification of the Vitamin D-response element (VDRE) in the Claudin-5 promoter**
210 To confirm the direct regulation of VDR on Claudin-5, we examined various models at the
211 basal level without any treatment *in vivo* and *in vitro*. In the $VDR^{-/-}$ mice, we observed that
212 these mice possessed lower Claudin-5 protein levels in the colon than did $VDR^{+/+}$ mice, and
213 TJ Claudin-7 was not altered in the absence of VDR (**Fig. S1A**). We further detected
214 significantly decreased mRNA levels of Claudin-5 in the intestines of $VDR^{-/-}$ mice (**Fig.**
215 **S1B**). The density of Claudin-5 fluorescence staining was weaker in the $VDR^{-/-}$ mouse
216 intestines (**Fig. S1C**). We also assessed the specificity of intestinal VDR in regulating
217 Claudin-5 expression in $VDR^{\Delta IEC}$ mice (**Fig. S1D**). Claudin-5 mRNA levels were significantly

218 reduced in $VDR^{\Delta IEC}$ mice compared to the levels in VDR-lox mice (**Fig. S1E**). As expected,
219 Claudin-7 expression remained unchanged. These data indicate that intestinal VDR
220 specifically regulates the expression level of Claudin-5 in the colon. To confirm our findings
221 *in vitro*, we used MEFs with VDR deletion. Lack of VDR led to a robust decrease in
222 Claudin-5 protein and mRNA levels in $VDR^{-/-}$ MEFs at the basal level (**Fig. S1F** and **S1G**).
223 The density of Claudin-5 fluorescence staining was also weaker in $VDR^{-/-}$ MEFs (**Fig. S1H**).
224
225 VDR acts as a transcription factor to regulate the expression of its target genes [30, 31].
226 Activated VDR binds to VDRE in the target gene promoter to regulate gene transcription
227 [32]. We reasoned that VDR may bind to the *Claudin-5 promoter* to thus alter the mRNA
228 expression of the Claudin-5 gene. Further, we performed a ChIP assay using the colon
229 mucosal extract from $VDR^{-/-}$ mice and nonspecific IgG as a negative control to assess the
230 binding of VDR to the Claudin-5 promoter. The samples were amplified by conventional
231 PCR using Ikβα as a positive control and Claudin-1 as a negative control as indicated in
232 previous publications [33]. CHIP-PCR demonstrated that VDR bound to the Claudin-5
233 promoter in the $VDR^{+/+}$ mouse colon **(Fig. 5A)**. The VDRE sequence
234 (AGTTCAAGTGGTTCT) within the Claudin-5 promoter region is shown in Figure **5B**.
235 However, siRNA-based Claudin-5 knock-down did not reduce VDR expression at the
236 mRNA level (**Fig. 5C)**. At the protein level, reduced Claudin-5 did not change the status of
237 VDR protein or Claudin-7 at the protein level (**Fig. 5D)**. These results suggest that VDR
238 transcriptionally regulates Claudin-5 at the mRNA level and that VDR is the upstream
239 regulator of Claudin-5.

High VDR levels led to increased Claudin-5 protein and mRNA levels *in vitro*.

We then explored the possibility of enhancing VDR to maintain the physiological level of Claudin-5**.** Vitamin D3 is known to increase VDR expression and to activate VDR signaling. We used the human colonic epithelial SKCO15 cell line that is widely used to study TJs [34, 35]. Claudin-5 mRNA level was significantly elevated in SKCO15 cells treated with vitamin D3, while Claudin-7 mRNA was not altered by vitamin D3 treatment (**Fig. 6A)**. The protein level of Claudin-5 was induced by vitamin D3 (**Fig. 6B**). *In vivo,* Claudin-5 mRNA levels were also increased in vitamin D3-treated mice (**Fig. 6C**). Colonoids are three-dimensional (3D) cell cultures that incorporate a number of key features of the colon [36]. In this study, we developed human colonoids (**Fig. 6E**), and we observed vitamin D3 treatment significantly increased Claudin-5 mRNA levels in these colonoids (**Fig. 6F**). Furthermore, vitamin D3 treatment significantly increased Claudin-5 protein levels in human colonoids, whereas there was no change of Claudin-7 after vitamin D3 treatment (**Fig. 6G**).

Intestinal epithelial VDR overexpression protected against the loss of Claudin 5 in respond to inflammation.

To further study the protective role of VDR in_maintaining TJs in inflammation, we generated a conditional intestinal epithelial VDR specific-overexpressed (O-VDR) mouse model. Epithelial VDR overexpression in mouse intestines significantly increased Claudin-5 expression at both the mRNA and protein levels (**Fig. 7A & B**). Claudin-5 exhibited a less decreaseat the mRNA and protein and mRNA levels in the colon of O-VDR mice treated

with DSS, compared to that in the O-VDR^{loxp} mice (**Fig. 7C &7D).** Using IF staining, we determined that Claudin-5 was better preserved in the colon of O-VDR mice treated with DSS compared to that in the O-VDR^{loxp} mice **(Fig. 7E &7G).** As anticipated**,** Claudin-7 expression was unchanged in the intestinal tissue of O-VDR mice that were treated with DSS compared to that in the O-VDR^{loxp} mice **(Fig. 7F).** VDR levels in fecal samples were detected using RT-PCR. VDR level was less decreased in DSS-treated O-VDR mice, compared to that in O-VDR^{loxp} mice treated with DSS **(Fig. 7H)**. Moreover, there were fewer inflammatory cytokines such as IL-1β and IL-17 in the colons of DSS-induced O-VDR mice compared to that in O-VDR^{loxp} mice **(Fig. 7I)**.

.

Discussion

In the current study, we determined that low colonic VDR expression was significantly correlated with the reduction of Claudin-5 in human CRC, and we demonstrated that VDR is important for the maintenance of cellular and physiological levels of TJ protein Claudin-5 in the colon to prevent inflammation and tumorigenesis. Our study further revealed a complex role for vitamin D/VDR regulation of *CLDN-5* in the development of colon cancer. Lack of VDR led to a reduction of Claudin-5 in tumors, and enhancing VDR increased Claudin-5 to protect the intestinal epithelial cells from tumorigenesis. At the molecular level, our data have demonstrated that the *CLDN-5* gene is a newly discovered downstream target of the transcriptional factor VDR. Overall, we noted a link between VDR signaling and barrier functions in CRC, thus suggesting a potential biomarker and target for a novel therapeutic strategy. Our study provides insight into how VDR signaling is involved in the tissue barrier related to tumorigenesis.

The intestinal barrier includes several elements that aid in its function as a physical and immunological barrier. These elements include the intestinal microbiota, secretory immunoglobulin A, antimicrobial peptides, the inner lamina propria, and epithelial cells. At the cellular level, epithelial cells play physical and physiological roles in health and disease. VDR signaling is involved in the epithelial barrier function related to various human diseases and remains largely unexplored [37]. As a nuclear receptor, VDR mediates most known functions of 1,25-dihydroxyvitamin D ($1,25(OH)_2D_3$), the active form of vitamin D [4]. However, the role of VDR has rarely been evaluated in studies examining human colon

296 cancer. A recent study among patients with digestive tract cancer and vitamin D
297 supplementation determined that when compared to placebo, this treatment did not result in
298 significant improvement in relapse-free survival at 5 years [38]. The dosage of vitamin D3
299 was insufficient among participants who possessed more severe deficiencies at baseline.
300 Therefore, the status of the VDR level must to be considered over the course of many trials
301 or as a biological measurement to clarify the underlying mechanisms. The traditional model
302 of treatment using vitamin D that guided early vitamin studies should give way to a model
303 incorporating more complex mechanisms of action of the vitamin D/VDR system. The
304 intestinal barrier has been investigated by various methods, but correlation of results across
305 studies is difficult, representing a major shortcoming in the field [39].
306
307 The current study provides important insights into how VDR regulates Claudin-5 expression
308 under normal physiological conditions and during tumor growth in the colon. We revealed a
309 positive correlation between VDR and Claudin-5 at the mRNA and protein levels in healthy
310 and tumor colons, thus suggesting the unique role of Claudin-5 in the intestine. There are
311 27 claudin family members that contribute to tight junctions [40], and not all claudins are the
312 same. Claudin-2- and Claudin-12 form paracellular Ca^{2+} channels in intestinal epithelia and
313 are important for vitamin D-dependent calcium homeostasis [41]. Our previous studies
314 have shown that Claudin-2 is hyperregulated in colitis with VDR reduction [42, 43]. Our
315 current study has demonstrated the mechanism on VDR-dependent function of Claudin-5 in
316 the intestine. Interestingly, we found that the tight junction Claudin-7 was not altered in
317 response to VDR-deficient status in the colon. In the lungs, VDR may play an important role

318 in maintaining the pulmonary barrier integrity. We have reported that VDR deletion could
319 increase lung permeability by altering the expression of TJ molecules, particularly
320 Claudin-2, -4, -10, -12, and -18 [44]. Abnormal gut barrier function may serve as a
321 biomarker for the risk of IBD onset [45]. Our findings also suggest that the positively
322 correlated status of VDR and Claudin-5 could be potentially applied to risk assessment,
323 early detection, and prevention of CRC, including colitis-associated colon cancer.
324
325 Colorectal cancer is the second-leading cause of cancer-related death and is most curable
326 in its early stages. Remarkable progress has been made in regard to colon cancer therapy,
327 including targeting barrier functions and microbiome [46]. The anti-TNF era has revealed
328 that mucosal healing is a key goal for therapy that predicts clinical remission and
329 resection-free survival in cancer patients. Many new targets (e.g., Jak inhibition, Toll-like
330 receptor 9 stimulation, and the addressin mucosal vascular addressin cell adhesion
331 molecule 1 emerge) have been recently tested for induction of mucosal healing and
332 protection and for induction and maintenance of remission in IBD. We aimed to provide a
333 detailed understanding of how VDR status contributes to changes in TJs in the context of
334 intestinal inflammation and colon cancer. Currently, there are no guidelines for monitoring
335 vitamin D status, treating hypovitaminosis D, and maintaining optimal vitamin D stores in
336 patients with IBD [47] or in CRC. These tasks may prove particularly difficult due to
337 malabsorption, gastrointestinal losses, and increased permeability that are associated with
338 intestinal dysfunction. Based on the research progress regarding the novel roles of VDR in
339 intestinal immunity and barrier functions, we expect that studies on VDR in intestinal

340 barriers of colitis and colon cancer will have a marked impact on the prevention, diagnosis,

341 and therapy of colitis and colon cancer patients.

342

Materials and Methods

Human tissue samples

This study was performed in accordance with approval from the University of Rochester Ethics Committee (RSRB00037178) and UIC Ethics Committee (Institutional Review Board: 2017-0384). Colorectal tissue samples were obtained from 10 CRC patients with neoplasia and 10 patients without neoplasia patients (49–74years old). Human tissues for organoids are from healthy volunteers.

Gene expression datasets

For expression analyses, we used microarray data reported in the NCBI Gene Expression Omnibus database (GEO). To find the correlation between VDR and Claudin-5 at the gene expression level, we gathered data by searching the Gene Expression Omnibus (https://www.ncbi.nlm.nih.gov/geo/) for expression profiling studies using colonic samples from colon cancer subjects. We randomly identified the GEO database reference series: GSE4183 [48] , GSE8671 [49], GSE10714 [50] and GSE37283) [51]. In these studies, the authors performed microarray analysis using colonic biopsy samples from healthy controls as well as from the inflamed and non-inflamed colonic mucosa from CRC subjects. From the databases, 40 healthy controls and 62 CRC patients were randomly selected for CRC group, while 16 healthy controls and 18 Colitis-associated CRC were randomly selected for colitis-associated group. Both were subjected to further analyses.

365 **Animals**

366 $VDR^{-/-}$ mice on a C57BL/6 background were obtained by breeding heterozygous $VDR^{+/-}$
367 mice[43]. $VDR^{\Delta IEC}$ mice were obtained by crossing the VDR^{LoxP-B} mice, originally provided
368 by Dr. Geert Carmeliet, with villin-cre mice (Jackson Laboratory, 004586), as we previously
369 reported [52].

370

371 Intestinal-specific VDR-overexpressing (O-VDR) mice were generated in C57BL/6 mice
372 strain background. The mouse VDR (mVDR) sequence was cloned into the Stbl3 vector
373 (size 6631 bp). The mVDR was cloned in (from ~2210 bp to ~3316bp) under EF1A
374 promoter (1bp to 1105bp). A LoxP site was integrated after EF1A promoter (from 1105 bp
375 to 2210 bp). VDR expression in O-VDR mice is Cre driven [53]. This $O\text{-}VDR^{loxp}$ mouse line
376 is labeled as $O\text{-}VDR^{loxp}$ in our gain of function study to distinct from the $VDR^{loxP/loxP}$ mouse
377 made for $VDR^{\Delta IEC}$ mice.

378

379 Experiments were performed on 2–3 months old mice including male and female. Mice
380 were provided with water ad libitum and maintained in a 12 h dark/light cycle. The animal
381 work was approved by the Rush University Animal Resources committee and UIC Office of
382 Animal Care. The animal work was approved by the UIC Office of Animal Care (ACC
383 15-231,17-218, and 18-216).

384

385 **Induction of colon cancer by AOM-DSS in mice**

386 Mice were treated with 10mg/kg of AOM (Sigma-Aldrich, Milwaukee, WI, USA) by
387 intraperitoneal injection as previously described [24]. After a 7-day recovery period, mice
388 received three cycles of 2% DSS in the drinking water. Tumor counts and measurements
389 were performed in a blinded fashion under a stereo-dissecting microscope (Nikon
390 SMZ1000, Melville, NY, USA). Microscopic analysis was performed for severity of
391 inflammation and dysplasia on hematoxylin and eosin-stained 'Swiss rolled' colons by a
392 gastrointestinal pathologist blinded to treatment conditions. Mice were scarified under
393 anaesthesia.
394
395 **Induction of colitis and experimental design**
396 Eight- to ten-week-old mice of a specific genetic background were grouped randomly into
397 control and DSS treatment groups. Colitis was induced by adding 5% (weight/volume)
398 dextran sodium sulfate (DSS) (mol. wt 36-50 kD; USB Corporation, Cleveland, OH, USA) to
399 the drinking water for 7 days. Mice were monitored regularly, and their body weights were
400 noted every day. All mice were provided a regular chow diet ad libitum. We checked the
401 effect of DSS on both OVDR mice and compared them with their respective control group.
402 On day 7, mice were sacrificed, and intestinal tissue and blood samples were harvested for
403 RNA, protein, immunofluorescence, and cytokine analysis as described in the results
404 section. The samples were immediately frozen and kept at -80°C until use.
405
406 **Vitamin D_3 treatment *in vivo***

C57/BL/6 wild-type mice (6-8-week-old males and females) were gavaged with 1,25 D_3 (0.2 μg/day in 100 μl of corn oil) 3 times a week for 4 weeks, as described in our previous study [54]. Intestinal tissue was collected following euthanasia.

Cell culture

Mouse embryonic fibroblasts (MEF) were isolated from embryonic day 13.5 embryos generated from $VDR^{+/-}$ x $VDR^{+/-}$ mouse breeding as previously described (32). $VDR^{+/+}$ and $VDR^{-/-}$ MEFs were used in experiments after more than 15 passages when they had been immortalized. MEFs and SKCO15 cells were grown in high glucose Dulbecco's Modified Eagle Medium (DMEM) (Hyclone, SH30243.01) containing 10% (v/v) fetal bovine serum (GEMINI, 900-108), 50 μg/ml streptomycin, and 50 U/ml penicillin (Mediatech, Inc., 30-002CI), as previously described [55].

Colonoids cultures and treatment with Vit D3

Human colonoids were prepared and maintained as previously described [56]. Mini gut medium (advanced DMEM/F12 supplemented with HEPES, L-glutamine, N2, and B27) was added to the culture, along with R-Spondin, Noggin, EGF, and Wnt-3a. At day 7 after passage, colonoids were treated by Vit D3 (20 nM) for indicated times.

Western blot analysis and antibodies

Mouse colonic epithelial cells were collected by scraping the tissue from the colon of the mouse, including the proximal and distal regions [52]. The cells were sonicated in lysis

429 buffer (10 mM Tris, pH 7.4, 150 mM NaCl, 1 mM EDTA, 1 mM EGTA, pH 8.0, 1% Triton
430 X-100) with 0.2 mM sodium ortho-vanadate, and protease inhibitor cocktail. The protein
431 concentration was measured using the BioRad Reagent (BioRad, Hercules, CA, USA).
432 Cultured cells were rinsed twice with ice-cold HBSS, lysed in protein loading buffer (50 mM
433 Tris, pH 6.8, 100 mM dithiothreitol, 2% SDS, 0.1% bromophenol blue, 10% glycerol), and
434 then sonicated. Equal amounts of protein were separated by SDS-polyacrylamide gel
435 electrophoresis, transferred to nitrocellulose, and immunoblotted with primary antibodies.
436 The following antibodies were used: anti-Claudin-5 (Invitrogen, 35-2500, Carlsbad, CA,
437 USA), anti-Claudin-7 (Invitrogen, 34-9100, Carlsbad, CA, USA), anti-VDR (Santa Cruz
438 Biotechnology, SC-13133, Dallas, TX, USA), anti-Villin (Santa Cruz Biotechnology,
439 SC-7672 Dallas, TX, USA), or anti-β-actin (Sigma-Aldrich, A5316, St. Louis, MO, USA)
440 antibodies and were visualized by ECL (Thermo Fisher Scientific, 32106, Waltham, MA,
441 USA). Membranes that were probed with more than one antibody were stripped before
442 re-probing.
443
444 **Immunofluorescence**
445 Colonic tissues were freshly isolated and embedded in paraffin wax after fixation with 10%
446 neutral buffered formalin. Immunofluorescence was performed on paraffin-embedded
447 sections (4 μm), after preparation of the slides as described previously [52], [55] followed by
448 incubation for 1 hour in blocking solution (2% bovine serum albumin, 1% goat serum in
449 HBSS) to reduce nonspecific background. The tissue samples were incubated overnight
450 with primary antibodies at 4°C. The following antibodies were used: anti-Claudin-5 and

anti-Claudin-7. Slides were washed 3 times for 5 minutes each at room temperature in wash buffer. Samples were then incubated with secondary antibodies (goat anti-rabbit Alexa Fluor 488, Molecular Probes, CA; 1:200) for 1 hour at room temperature. Tissues were mounted with SlowFade Antifade Kit (Life technologies, s2828, Grand Island, NY, USA), followed by a coverslip, and the edges were sealed to prevent drying. Specimens were examined with a Zeiss laser scanning microscope LSM 710 (Carl Zeiss Inc., Oberkochen, Germany).

Immunohistochemistry (IHC)

After preparation of the slides, antigen retrieval was achieved by incubation of the slides for 15 min in the hot preheating sodium citrate (pH 6.0) buffer, and 30 min of cooling at room temperature. Endogenous peroxidases were quenched by incubating the slides in 3% hydrogen peroxide for 10 min, followed by three rinses with HBSS, and incubation for 1 hour in 3% BSA + 1% goat serum in HBSS to reduce nonspecific background. Primary antibodies VDR (1:300) was applied for overnight in a cold room. After three rinses the slides with HBSS, they were incubated in secondary antibody (1:100, Jackson ImmunoResearch Laboratories, Cat.No.115-065-174, West Grove, PA, USA) for 1 hour at room temperature. After washing with HBSS for 10 minutes, the slides were incubated with vectastain ABC reagent (Vector Laboratories, Cat.No. PK-6100, Burlingame, CA 94010, USA) for 1 hour. After washing with HBSS for five minutes, color development was achieved by applying peroxidase substrate kit (Vector Laboratories, Cat.No. SK-4800, Burlingame, CA 94010) for 2 to 5 minutes, depending on the primary antibody. The duration

of peroxidase substrate incubation was determined through pilot experiments and was then held constant for all of the slides. After washing in distilled water, the sections were counterstained with haematoxylin (Leica, Cat.No.3801570, Wetzlar, Germany), dehydrated through ethanol and xylene, and cover-slipped using a permount (Fisher Scientific, Cat.No.SP15-100, Waltham, MA, USA).

Real Time quantitative PCR

Total RNA was extracted from epithelial cell monolayers or mouse colonic epithelial cells using TRIzol reagent (Fisher Scientific, 15596026, Waltham, MA, USA) [52]. RNA reverse transcription was done using the iScript cDNA synthesis kit (Bio-Rad Laboratories, 1708891) according to the manufacturer's directions. The RT-cDNA reaction products were subjected to quantitative real-time PCR using the CFX96 Real time PCR detection system (Bio-Rad Laboratories, Hercules, CA, USA) and iTaq^{TM} Universal SYBR green supermix (Bio-Rad Laboratories, 1725121, Hercules, CA, USA) according to the manufacturer's directions. All expression levels were normalized to β-actin levels of the same sample. Percent expression was calculated as the ratio of the normalized value of each sample to that of the corresponding untreated control cells. All real-time PCR reactions were performed in triplicate. Primer sequences were designed using Primer-BLAST or were obtained from Primer Bank primer pairs listed in **Table 1**.

Chromatin immunoprecipitation (CHIP) assay

494 Binding of VDR to the Claudin-5 promoter was investigated using the ChIP assay as
495 described previously [57]. Briefly, mouse colonic epithelial cells were collected by scraping
496 the tissue from the colon of the mouse, cells were treated with 1% formaldehyde for 10 min
497 at 37°C. Cells were washed twice in ice-cold phosphate buffered saline containing protease
498 inhibitor cocktail tablets. Cells were scraped into conical tubes, pelleted and lysed in SDS
499 Lysis Buffer. The lysate was sonicated to shear DNA into fragments of 200–1000 bp (4
500 cycles of 10 s sonication, 10 s pausing, Branson Sonifier 250, USA). The chromatin
501 samples were pre-cleared with salmon sperm DNA–bovine serum albumin-sepharose
502 beads, then incubated overnight at 4 °C with VDR antibody. Immune complexes were
503 precipitated with salmon sperm DNA-bovine serum albumin-sepharose beads. DNA was
504 prepared by treatment with proteinase K, extraction with phenol and chloroform, and
505 ethanol precipitation.
506
507 **Multiplex ELISA assay**
508 A mouse-specific ProcartaIPlex™ Multiplex Immunoassay (26) plate from Invitrogen
509 Thermo Fisher Scientific was used to detect serum cytokine levels. The assay was
510 performed using the manufacturer's instruction manual using proper standards. Eventually,
511 the plate was read using a Megpix Luminex machine.
512
513 **Test fecal VDR by PCR**
514 Total RNA was extracted from mouse fecal samples, as previously described.[58] Briefly,
515 About 100 mg of Frozen fecal pellet was used for RNA extraction by using Trizol Reagent

(Thermo Fisher Scientific, Cat.No.15596018, Waltham, MA, USA). To increase RNA yield in high quality, RNeasy minispin column (Qiagen, Cat No.217004, Hilden, Germany) was used by following the manufacturer's instructions.

Statistical Analysis

All data are expressed as the mean ± SD. All statistical tests were 2-sided. All *p* values < 0.05 were considered statistically significant. After the Shapiro-Wilk test confirmed that the data are normally distributed, the differences between samples were analyzed using unpaired *t* test for two groups and using one-way ANOVA for more than two groups as appropriate, respectively. The *p* values in ANOVA analysis and generalized linear mixed models were adjusted using the Tukey method to ensure accurate results. Pairwise correlation analyses and scatter plots were conducted staining intensity changes between VDR protein and Claudin-5, using SAS version 9.4 (SAS Institute, Inc., Cary, NC, USA). Other statistical analyses were performed using GraphPad Prism 6 (GraphPad, Inc., San Diego, CA., USA).

Tables

Table 1: Real-time PCR Primers

Primers name	Sequence
mβ-actinF	5′-TGTTACCAACTGGGACGACA-3′
mβ-actinR	5′-CTGGGTCATCTTTTCACGGT-3′
mVDRF	5′-GAATGTGCCTCGGATCTGTGG-3′
mVDRR	5′-ATGCGGCAATCTCCATTGAAG-3′
mClaudin-5F	5′- AGGCACGGGTAGCACTCACG-3′
mClaudin-5R	5′- CATAGTTCTTCTTGTCGTAATC-3′
mClaudin-7F	5′-GCGACAACATCATCACAGCC-3′
mClaudin-7R	5′-CCTTGGAGGAATTGGACTTGG-3′
mTNF-α F	5′-CCCTCACACTCAGATCATCTTCT-3′
mTNF-α R	5′-GCTACGACGTGGGCTACAG-3′
mIL-1βF	5′-GCAACTGTTCCTGAACTCAACT-3′
mIL-1βR	5′-ATCTTTTGGGGTCCGTCAACT-3′
mIL-17F	5′-TTTAACTCCCTTGGCGCAAAA-3′
mIL-17R	5′-CTTTCCCTCCGCATTGACAC-3′
hβ-actinF	5′-AGAGCAAGAGAGGCATCCTC-3′
hβ-actinR	5′-CTCAAACATGATCTGGGTCA-3′
hVDRF	5′-GGACTGCCGCATCACCAA-3′
hVDRR	5′-TCATCTCCCGCTTCCTCT-3′
hClaudin-5F	5′-TTCGCCAACATTGTCGTCC-3′
hClaudin-5R	5′-TCTTCTTGTCGTAGTCGCCG-3′
hClaudin-7F	5′-CATCGTGGCAGGTCTTGCC-3′
hClaudin-7R	5′-GATGGCAGGGCCAAACTCATAC-3′

Figure Legends

Fig. 1 Reduced VDR was correlated with low Claudin-5 expression in human CRC patients

(A) Reduced VDR and Claudin-5 expression in patients with CRC (GEO database GSE4183 and GSE8671 (data were expressed as mean ± SD; Normal, n=40; CRC, n=62; student t test, * P < 0.05). **(B)** Significantly coordinated expression of VDR and Claudin-5 in biopsy samples collected from CRC patients. We performed a regression of VDR against Claudin-5 and conducted a scatter plot analysis with a regression line (GEO database GSE4183 and GSE8671, Normal, n=40; CRC, n=62; Intercept = 0.244; Slope = 0.5297). Values for healthy controls are presented in blue and values for CRC patients are presented in red. **(C)** Reduced VDR and Claudin-5 expression in patients with Colitis-associated CRC (GEO database GSE8671, GSE10714 and GSE37283 (data were expressed as mean ± SD; Normal, n=16; Colitis-associated CRC, n=18; student t test, * P < 0.05). **(D)** Coordinated expression of VDR and Claudin-5 in biopsy samples collected from Colitis-associated CRC patients. We performed a regression of VDR against Claudin-5 and conducted a scatter plot analysis with a regression line (GEO database GSE8671, GSE10714 and GSE37283 Normal, n=16; Colitis-associated CRC, n=18; the correlation is 0.2549 with p-value = 0.1457). **(E)** Intestinal VDR staining in normal and CRC human colon samples. Compared to normal intestines, intestines from CRC patients possessed significantly lower VDR expression. (Images are representative of experiments performed in triplicate; Normal, n=10; Colorectal cancer, n=10; Student *t* test; *P < 0.05). **(F)** IF staining of Claudin-5 in normal and CRC human colon samples. Compared to normal

intestines, the intestines of CRC patients exhibited significantly lower Claudin-5 expression. (Images are representative of experiments in triplicate; Normal, n=10; Colon cancer, n=10; Student *t* test; **P* < 0.05). **(G)** The correlation analysis of staining intensity between intestinal Claudin-5 and VDR in human colon samples. (P < 0.0734, n = 6 for Normal and Colon cancer, respectively).

Fig. 2 $VDR^{-/-}$ mice developed a greater number of tumors compared to tumors in $VDR^{+/+}$ mice.

(A) Schematic overview of the AOM/DSS-induced colon cancer model. AOM (10 mg/kg) was injected on day 0. At Day 7, 2% DSS solution was administered to mice in drinking water. Seven days of DSS was followed by three weeks of drinking water that was free of DSS. An additional two cycles of DSS were administered prior to scarification at Week 19. **(B)** Colonic tumors *in situ*. Representative colons from different groups. Tumors are indicated by red arrows. **(C)** Tumor numbers in AOM-DSS-induced colon cancer model: $VDR^{+/+}$ and $VDR^{-/-}$ mice (data are expressed as mean ± SD. n = 10-13, one-way ANOVA test, *P < 0.05). **(D)** Max tumor size in AOM-DSS induced colon cancer model: $VDR^{+/+}$ and $VDR^{-/-}$ mice (data are expressed as mean ± SD. n = 10-13, one-way ANOVA test, *P < 0.05). **(E)** Representative H&E staining of “Swiss rolls” of representative colons from the indicated groups. Images are from a single experiment and are representative of 10 mice per group. **(F)** Quantitation of PCNA-positive cells in control mucosa per intestinal glands or in the tumors tissue per high-power field. PCNA expression in the tumor tissue of $VDR^{-/-}$ mice was significantly higher, compared to that in the $VDR^{+/+}$ mice (data are

580 expressed as mean ± SD. n = 5, student's t-test, *P < 0.05). **(G)** Serum cytokines such as
581 TNF-α, IL-1β, and IL-17 were significantly increased, particularly in the AOM-DSS-induced
582 $VDR^{-/-}$ mice colon cancer model. Each single experiment was assayed in triplicate. Data are
583 expressed as mean ± SD. n = 6, one-way ANOVA test, *P < 0.05.
584
585 **Fig. 3 VDR deletion led to decreased Claudin-5 expression in tumor tissues**
586 **(A)** Intestine permeability increased in the AOM-DSS-induced $VDR^{-/-}$ mice colon cancer
587 model. Fluorescein Dextran (Molecular weight 3 kDa, diluted in HBSS) was gavaged (50
588 mg/g mouse). Four hours later, mouse blood samples were collected for fluorescence
589 intensity measurement (data are expressed as mean ± SD; n = 5 mice/group, 1-way
590 ANOVA test; *P < 0.05). **(B)** VDR deletion decreased Claudin-5 at the mRNA level in the
591 colon (data are expressed as mean ± SD. n = 5, one-way ANOVA test, *P < 0.05). **(C)** VDR
592 deletion decreased Claudin-5 at the protein level in the colon (data are expressed as mean
593 ± SD. n = 5, one-way ANOVA test, *P < 0.05). (**D**) **(G)** Claudin-5 was decreased in the
594 tumor tissue of $VDR^{-/-}$ mice, compared to levels in the tumor tissue of $VDR^{+/+}$ mice
595 according to immunofluorescence staining. Images are from a single experiment and are
596 representative of 6 mice per group. (Data are expressed as mean ± SD. n = 6, one-way
597 ANOVA test, *P < 0.05). **(E)** Claudin-7 was unchanged in the tumor tissue of $VDR^{-/-}$ mice
598 compared to levels in the tumor tissue of $VDR^{+/+}$ mice according to immunofluorescence
599 staining. Images are from a single experiment and are representative of 6 mice per group.
600 **(F)(H)** Intestinal VDR expression was decreased in the AOM-DSS-induced colon cancer
601 model. Images are from a single experiment and are representative of 6 mice per group.

602 Data are expressed as mean ± SD. n = 6, one-way ANOVA test, *P < 0.05). **(I)** VDR levels
603 in fecal samples were detected using RT-PCR. VDR expression was downregulated in the
604 AOM-DSS-treated $VDR^{+/+}$ mice (data are expressed as mean ± SD. *n* = 5, one-way
605 ANOVA test, *P < 0.05).
606
607 **Fig. 4 VDR-specific deletion in mouse intestines lead to decreased Claudin-5**
608 **expression in tumor tissues**
609 **(A)** Intestine permeability was increased in the AOM-DSS-induced $VDR^{\Delta IEC}$ mice colon
610 cancer model (data are expressed as mean ± SD; n = 5 mice/group, 1-way ANOVA test;
611 *P < 0.05). **(B)** VDR-specific deletion in mouse intestines decreased Claudin-5 at the
612 mRNA level in the colon (data are expressed as mean ± SD. n = 5, one-way ANOVA test,
613 *P < 0.05). **(C)** VDR-specific deletion in mouse intestines decreased Claudin-5 protein in
614 the colon (data are expressed as mean ± SD. n = 5, one-way ANOVA test, *P < 0.05). **(D)**
615 Claudin-5 was decreased in the tumor tissue of $VDR^{\Delta IEC}$ mice compared to levels in the
616 tumor tissue of VDR^{loxp} mice according to immunofluorescence staining. Images are from a
617 single experiment and are representative of 6 mice per group. **(E)** Claudin-7 expression
618 was not changed in the AOM-DSS-induced VDR^{loxp} mice colon cancer model. Images are
619 from a single experiment and are representative of 6 mice per group. (**F**) Intensity of the
620 staining of Claudin-5. (Data are expressed as mean ± SD. n = 6, one-way ANOVA test,
621 *P < 0.05). **(G)** VDR level in fecal samples was detected by RT-PCR. VDR expression was
622 downregulated in the AOM-DSS-treated VDR^{loxp} mice (data are expressed as
623 mean ± SD. *n* = 3, one-way ANOVA test, *P < 0.05).

Fig. 5. VDR binds to the Claudin-5 promoter *in vivo* and *in vitro*

(A) CHIP-PCR amplification demonstrated that VDR binds to the promoter regions of Claudin-5 in mouse colons. PCR assays were performed and included input-positive controls and IgG/villin-negative controls. n = 3 separate experiments. **(B)** Claudin-5 promoter regions with VDRE sequence. (**C**) Claudin-5 knockdown using siRNA (40 nM for 72 hours) did not reduce VDR expression at the mRNA level. (Data are expressed as mean ± SD. *n* = 3, one-way ANOVA test, *P < 0.05). (**D**) The protein expression in SKCO15 cells using siRNA (40 nM for 72 hours). (data are expressed as mean ± SD. *n* = 3, one-way ANOVA test, *P < 0.05).

Fig. 6. High VDR levels led to increased Claudin-5 at the protein and mRNA levels *in vitro*.

(A) Claudin-5 mRNA and (**B**) protein levels were increased after 24-hour vitamin D3 treatment at 20 nM in SKCO15 cells (data are expressed as mean ± SD. student's t-test, *P < 0.05. n = 3). **(C)** Claudin-5 mRNA and **(D)** protein levels were higher in vitamin D3-treated $VDR^{+/+}$ mice. $VDR^{+/+}$ mice (6-8 weeks) were gavaged by 0.2 µg vitamin D3 in 0.1 ml corn oil for 3 times per week for 4 weeks (data are expressed as mean ± SD. student's t-test, *P < 0.05. n= 5 mice / group). **(E)** The micrographs show representative human colonoids that were treated with Vit D_3 (20 nM) for the indicated time points. **(F)** Claudin-5 mRNA and (**G**) protein levels were increased after vitamin D3 treatment in

human colonoids (data are expressed as mean ± SD, n= 5, one-way ANOVA test, *P < 0.05).

Fig. 7. Overexpressed intestinal epithelial VDR led to increased Claudin-5 and reduced inflammation *in vivo*.

(A) VDR overexpression in mice intestines increased Claudin-5 expression in the colon at the mRNA and (B) protein levels (data are expressed as mean ± SD. n = 3, one-way ANOVA test, *P < 0.05). **(C)** Claudin-5 was less decreased at the mRNA and (**D**) protein levels in the intestinal tissue of O-VDR mice treatment with DSS compared to levels in the O-VDR^{loxp} mice (data are expressed as mean ± SD. n = 3, one-way ANOVA test, *P < 0.05). **(E)** Claudin-5 was less decreased in the intestinal tissue of O-VDR mice treated with DSS compared to levels in the O-VDR^{loxp} mice, according to immunofluorescence staining. Images are from a single experiment and are representative of 5 mice per group. **(F)** Claudin-7 was unchanged in the intestinal tissue of O-VDR mice treated with DSS compared to levels in the O-VDR^{loxp} mice according to immunofluorescence staining. Images are from a single experiment and are representative of 5 mice per group. **(G)** Intensity of the staining of Claudin-5. Images are from a single experiment and are representative of 5 mice per group. (Data are expressed as mean ± SD. n = 5, one-way ANOVA test, *P < 0.05). **(H)** VDR level in fecal samples was detected by RT-PCR. VDR expression was less decreased in O-VDR mice treated with DSS compared to levels in the O-VDR^{loxp} mice treated with DSS (data are expressed as mean ± SD. *n* = 3, one-way ANOVA test, *P < 0.05). **(I)** The inflammatory cytokines IL-1β and IL-17 were less

667 increased in the DSS-induced O-VDR mice colitis model compare to levels in O-VDR^{loxp}

668 mice (data are expressed as mean ± SD. *n* = 3, one-way ANOVA test, *P < 0.05).

669

Fig. S1. VDR deficiency in intestinal epithelial cells of mice leads to the reduction of Claudin-5 at both the mRNA and protein levels *in vivo*.

(A) Claudin-5 protein and **(B)** mRNA levels were significantly lower in $VDR^{-/-}$ mice compared to levels in the $VDR^{+/+}$ mice (data are expressed as mean ± SD. n = 5, student's t-test, *P < 0.05). **(C)** Location of Claudin-5 protein in the colons of $VDR^{+/+}$ and $VDR^{-/-}$ mice. Images are from a single experiment and are representative of 5 mice per group. **(D)** Claudin-5 protein and **(E)** mRNA levels were significantly lower in $VDR^{\Delta IEC}$ mice compared to levels in the VDR^{loxp} mice (data are expressed as mean ± SD. n = 5, student's t-test, *P < 0.05). **(F)** Claudin-5 protein and **(G)** mRNA were both decreased in $VDR^{-/-}$ MEF cells (data are expressed as mean ± SD. n = 3, student's t-test, *P < 0.05). **(H)** Location and quantification of Claudin-5 protein in $VDR^{+/+}$ and $VDR^{-/-}$ MEF cells. Images are from a single experiment performed in triplicate. (Data are expressed as mean ± SD. n = 3, one-way ANOVA test, *P < 0.05).

References

1 Zeissig S, Burgel N, Gunzel D, Richter J, Mankertz J, Wahnschaffe U*, et al.* Changes in expression and distribution of claudin 2, 5 and 8 lead to discontinuous tight junctions and barrier dysfunction in active Crohn's disease. Gut 2007;**56**:61-72.

2 Zhu L, Han J, Li L, Wang Y, Li Y, Zhang S. Claudin Family Participates in the Pathogenesis of Inflammatory Bowel Diseases and Colitis-Associated Colorectal Cancer. Frontiers in immunology 2019;**10**:1441.

3 Cherradi S, Martineau P, Gongora C, Del Rio M. Claudin gene expression profiles and clinical value in colorectal tumors classified according to their molecular subtype. Cancer management and research 2019;**11**:1337-48.

4 Haussler MR, Whitfield GK, Haussler CA, Hsieh J-C, Thompson PD, Selznick SH*, et al.* The nuclear vitamin D receptor: biological and molecular regulatory properties revealed. J Bone and Mineral Research 1998;**13**:325-49.

5 Xue Y, Fleet JC. Intestinal vitamin D receptor is required for normal calcium and bone metabolism in mice. Gastroenterology 2009;**136**:1317-27, e1-2.

6 Bouillon R, Carmeliet G, Verlinden L, van Etten E, Verstuyf A, Luderer HF*, et al.* Vitamin D and human health: lessons from vitamin D receptor null mice. Endocr Rev 2008;**29**:726-76.

7 Ogura M, Nishida S, Ishizawa M, Sakurai K, Shimizu M, Matsuo S*, et al.* Vitamin D3 modulates the expression of bile acid regulatory genes and represses inflammation in bile duct-ligated mice. J Pharmacol Exp Ther 2009;**328**:564-70.

8 Kamen DL, Tangpricha V. Vitamin D and molecular actions on the immune system: modulation of innate and autoimmunity. J Mol Med;**88**:441-50.

9 Waterhouse JC, Perez TH, Albert PJ. Reversing bacteria-induced vitamin D receptor dysfunction is key to autoimmune disease. Ann N Y Acad Sci 2009;**1173**:757-65.

10 Liu PT, Krutzik SR, Modlin RL. Therapeutic implications of the TLR and VDR partnership. Trends Mol Med 2007;**13**:117-24.

11 Gombart AF, Borregaard N, Koeffler HP. Human cathelicidin antimicrobial peptide (CAMP) gene is a direct target of the vitamin D receptor and is strongly up-regulated in myeloid cells by 1,25-dihydroxyvitamin D3. FASEB J 2005;**19**:1067-77.

12 Kong J, Zhang Z, Musch MW, Ning G, Sun J, Hart J*, et al.* Novel role of the vitamin D receptor in maintaining the integrity of the intestinal mucosal barrier. Am J Physiol Gastrointest Liver Physiol 2008;**294**:G208-16.

13 Adams JS, Hewison M. Unexpected actions of vitamin D: new perspectives on the regulation of innate and adaptive immunity. Nat Clin Pract Endocrinol Metab 2008;**4**:80-90.

14 Yu S, Bruce D, Froicu M, Weaver V, Cantorna MT. Failure of T cell homing, reduced CD4/CD8alphaalpha intraepithelial lymphocytes, and inflammation in the gut of vitamin D receptor KO mice. Proceedings of the National Academy of Sciences of the United States of America 2008;**105**:20834-9.

15 Lloyd-Price J, Arze C, Ananthakrishnan AN, Schirmer M, Avila-Pacheco J, Poon TW*, et al.* Multi-omics of the gut microbial ecosystem in inflammatory bowel diseases. Nature 2019;**569**:655-62.

16 Abreu MT, Kantorovich V, Vasiliauskas EA, Gruntmanis U, Matuk R, Daigle K*, et al.* Measurement of vitamin D levels in inflammatory bowel disease patients reveals a subset of Crohn's disease patients with elevated 1,25-dihydroxyvitamin D and low bone mineral density. Gut 2004;**53**:1129-36.

17 Lim WC, Hanauer SB, Li YC. Mechanisms of disease: vitamin D and inflammatory bowel disease. Nat Clin Pract Gastroenterol Hepatol 2005;**2**:308-15.

18 Wang TT, Dabbas B, Laperriere D, Bitton AJ, Soualhine H, Tavera-Mendoza LE*, et al.* Direct and indirect induction by 1,25-dihydroxyvitamin D3 of the NOD2/CARD15-defensin beta2 innate immune pathway defective in Crohn disease. The Journal of biological chemistry;**285**:2227-31.

19 Rufo PA, Bousvaros A. Current therapy of inflammatory bowel disease in children. Paediatr Drugs 2006;**8**:279-302.

20 Sun J. Vitamin D and mucosal immune function. Curr Opin Gastroenterol 2010;**26**:591-5.

21 Song M, Chan AT, Jun J. Features of the Gut Microbiome, Diet, and Environment That Influence Risk of Colorectal Cancer. Gastroenterology 2020.

22 Lu R, Zhang Y, Xia Y, Zhang J, Kaser A, Blumberg R*, et al.* Paneth cell alertness to pathogens maintained by vitamin D receptors. Gastroenterology 2020.

23 Zhang Y-G, Lu R, Wu S, Chatterjee I, Zhou D, Xia Y*, et al.* Vitamin D receptor protects against dysbiosis and tumorigenesis via the JAK/STAT pathway in intestine. Biorxiv 2020;**02**.

24 Zhang YG, Lu R, Wu S, Chatterjee I, Zhou D, Xia Y*, et al.* Vitamin D Receptor Protects Against Dysbiosis and Tumorigenesis via the JAK/STAT Pathway in Intestine. Cell Mol Gastroenterol Hepatol 2020;**10**:729-46.

25 Wong SH, Zhao L, Zhang X, Nakatsu G, Han J, Xu W*, et al.* Gavage of Fecal Samples From Patients With Colorectal Cancer Promotes Intestinal Carcinogenesis in Germ-Free and Conventional Mice. Gastroenterology 2017;**153**:1621-33 e6.

26 Andoh A, Imaeda H, Aomatsu T, Inatomi O, Bamba S, Sasaki M*, et al.* Comparison of the fecal microbiota profiles between ulcerative colitis and Crohn's disease using terminal restriction fragment length polymorphism analysis. J Gastroenterol 2011;**46**:479-86.

27 Bird RP, Good CK. The significance of aberrant crypt foci in understanding the pathogenesis of colon cancer. Toxicol Lett 2000;**112-113**:395-402.

28 Kang X, Zhang R, Kwong TN, Lui RN, Wu WK, Sung JJ*, et al.* Serrated neoplasia in the colorectum: gut microbiota and molecular pathways. Gut Microbes 2021;**13**:1-12.

29 Yongguo Zhang YX, Jun Sun. . A simple and sensitive method to detect vitamin D receptor expression in various disease models using stool samples. Genes and Diseases 2020.

30 Wu S, Zhang YG, Lu R, Xia Y, Zhou D, Petrof EO*, et al.* Intestinal epithelial vitamin D receptor deletion leads to defective autophagy in colitis. Gut 2015;**64**:1082-94.

31 Sun J, Kong J, Duan Y, Szeto FL, Liao A, Madara JL*, et al.* Increased NF-kappaB activity in fibroblasts lacking the vitamin D receptor. Am J Physiol Endocrinol Metab 2006;**291**:E315-22.

32 Kato S. The function of vitamin D receptor in vitamin D action. J Biochem 2000;**127**:717-22.

33 Zhang Y-g, Wu S, Lu R, Zhou D, Zhou J, Carmeliet G*, et al.* Tight junction CLDN2 gene is a direct target of the vitamin D receptor. Scientific Reports 2015;**5**:10642.

34 Capaldo CT, Koch S, Kwon M, Laur O, Parkos CA, Nusrat A. Tight function zonula occludens-3 regulates cyclin D1-dependent cell proliferation. Molecular biology of the cell 2011;**22**:1677-85.

35 Ivanov AI, McCall IC, Babbin B, Samarin SN, Nusrat A, Parkos CA. Microtubules regulate disassembly of epithelial apical junctions. BMC cell biology 2006;**7**:12.

36 Zhang YG, Zhu X, Lu R, Messer JS, Xia Y, Chang EB*, et al.* Intestinal epithelial HMGB1 inhibits bacterial infection via STAT3 regulation of autophagy. Autophagy 2019;**15**:1935-53.

37 Zhang YG, Wu S, Sun J. Vitamin D, Vitamin D Receptor, and Tissue Barriers. Tissue barriers 2013;**1**.

38 Urashima M, Ohdaira H, Akutsu T, Okada S, Yoshida M, Kitajima M*, et al.* Effect of Vitamin D Supplementation on Relapse-Free Survival Among Patients With Digestive Tract Cancers: The AMATERASU Randomized Clinical Trial. JAMA 2019;**321**:1361-9.

39 Vancamelbeke M, Vermeire S. The intestinal barrier: a fundamental role in health and disease. Expert Rev Gastroenterol Hepatol 2017;**11**:821-34.

40 Mineta K, Yamamoto Y, Yamazaki Y, Tanaka H, Tada Y, Saito K*, et al.* Predicted expansion of the claudin multigene family. FEBS Letters 2011;**585**:606-12.

41 Fujita H, Sugimoto K, Inatomi S, Maeda T, Osanai M, Uchiyama Y*, et al.* Tight junction proteins claudin-2 and -12 are critical for vitamin D-dependent Ca2+ absorption between enterocytes. Molecular biology of the cell 2008;**19**:1912-21.

42 Zhang YG, Lu R, Xia Y, Zhou D, Petrof E, Claud EC*, et al.* Lack of Vitamin D Receptor Leads to Hyperfunction of Claudin-2 in Intestinal Inflammatory Responses. Inflamm Bowel Dis 2019;**25**:97-110.

43 Zhang YG, Wu S, Lu R, Zhou D, Zhou J, Carmeliet G*, et al.* Tight junction CLDN2 gene is a direct target of the vitamin D receptor. Sci Rep 2015;**5**:10642.

44 Chen H, Lu R, Zhang YG, Sun J. Vitamin D Receptor Deletion Leads to the Destruction of Tight and Adherens Junctions in Lungs. Tissue barriers 2018;**6**:1-13.

45 Turpin W, Lee SH, Raygoza Garay JA, Madsen KL, Meddings JB, Bedrani L*, et al.* Increased Intestinal Permeability is Associated with Later Development of Crohn's Disease. Gastroenterology 2020.

46 Wong SH, Yu J. Gut microbiota in colorectal cancer: mechanisms of action and clinical applications. Nat Rev Gastroenterol Hepatol 2019;**16**:690-704.

47 Pappa HM, Grand RJ, Gordon CM. Report on the vitamin D status of adult and pediatric patients with inflammatory bowel disease and its significance for bone health and disease. Inflamm Bowel Dis 2006;**12**:1162-74.

48 Galamb O, Gyorffy B, Sipos F, Spisak S, Nemeth AM, Miheller P*, et al.* Inflammation, adenoma and cancer: objective classification of colon biopsy specimens with gene expression signature. Disease markers 2008;**25**:1-16.

812 49 Sabates-Bellver J, Van der Flier LG, de Palo M, Cattaneo E, Maake C, Rehrauer
813 H*, et al.* Transcriptome profile of human colorectal adenomas. Molecular cancer research :
814 MCR 2007;**5**:1263-75.
815 50 Galamb O, Sipos F, Solymosi N, Spisak S, Krenacs T, Toth K*, et al.* Diagnostic
816 mRNA expression patterns of inflamed, benign, and malignant colorectal biopsy specimen
817 and their correlation with peripheral blood results. Cancer epidemiology, biomarkers &
818 prevention : a publication of the American Association for Cancer Research, cosponsored
819 by the American Society of Preventive Oncology 2008;**17**:2835-45.
820 51 Pekow J, Dougherty U, Huang Y, Gometz E, Nathanson J, Cohen G*, et al.* Gene
821 signature distinguishes patients with chronic ulcerative colitis harboring remote neoplastic
822 lesions. Inflamm Bowel Dis 2013;**19**:461-70.
823 52 Zhang H, Wu H, Liu L, Li H, Shih DQ, Zhang X. 1,25-dihydroxyvitamin D3
824 regulates the development of chronic colitis by modulating both T helper (Th)1 and Th17
825 activation. APMIS 2015;**123**:490-501.
826 53 Chatterjee I, Zhang Y, Zhang J, Lu R, Xia Y, Sun J. Overexpression of Vitamin D
827 Receptor in Intestinal Epithelia Protects Against Colitis via Upregulating Tight Junction
828 Protein Claudin 15. Journal of Crohn's and Colitis 05 March, 2021.
829 54 Lu R, Zhang YG, Xia Y, Sun J. Imbalance of autophagy and apoptosis in intestinal
830 epithelium lacking the vitamin D receptor. FASEB J 2019:fj201900727R.
831 55 Lu R, Wu S, Liu X, Xia Y, Zhang YG, Sun J. Chronic effects of a Salmonella type III
832 secretion effector protein AvrA in vivo. PLoS One 2010;**5**:e10505.
833 56 Lu R, Voigt RM, Zhang Y, Kato I, Xia Y, Forsyth CB*, et al.* Alcohol Injury Damages
834 Intestinal Stem Cells. Alcoholism, clinical and experimental research 2017;**41**:727-34.
835 57 Wu S, Xia Y, Liu X, Sun J. Vitamin D receptor deletion leads to reduced level of
836 IkappaBalpha protein through protein translation, protein-protein interaction, and
837 post-translational modification. Int J Biochem Cell Biol 2010;**42**:329-36.
838 58 Zhang Y-g, Xia Y, Sun J. A simple and sensitive method to detect vitamin D
839 receptor expression in various disease models using stool samples. Genes & Diseases
840 2020.
841

Figure.1

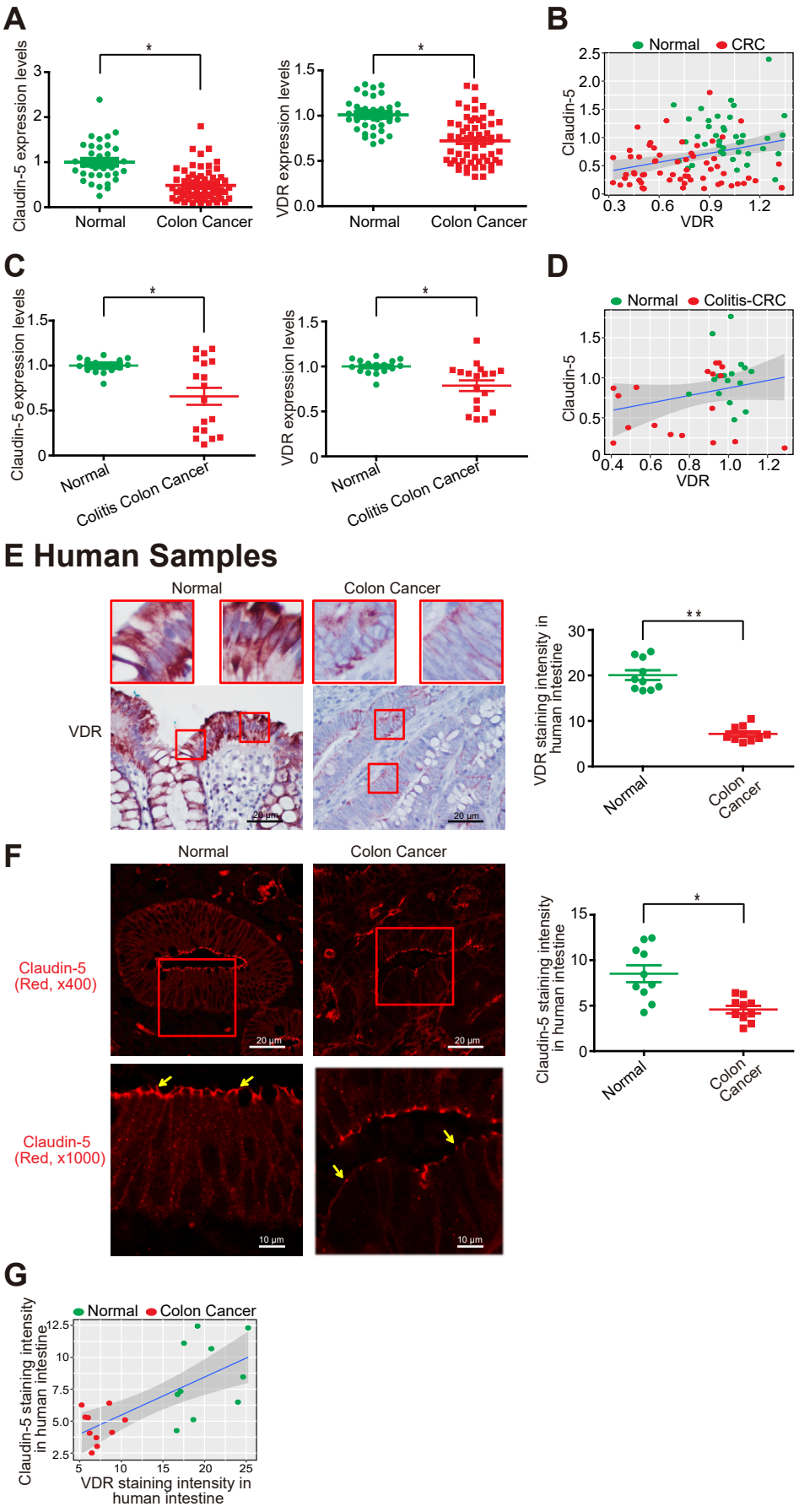

Figure.2

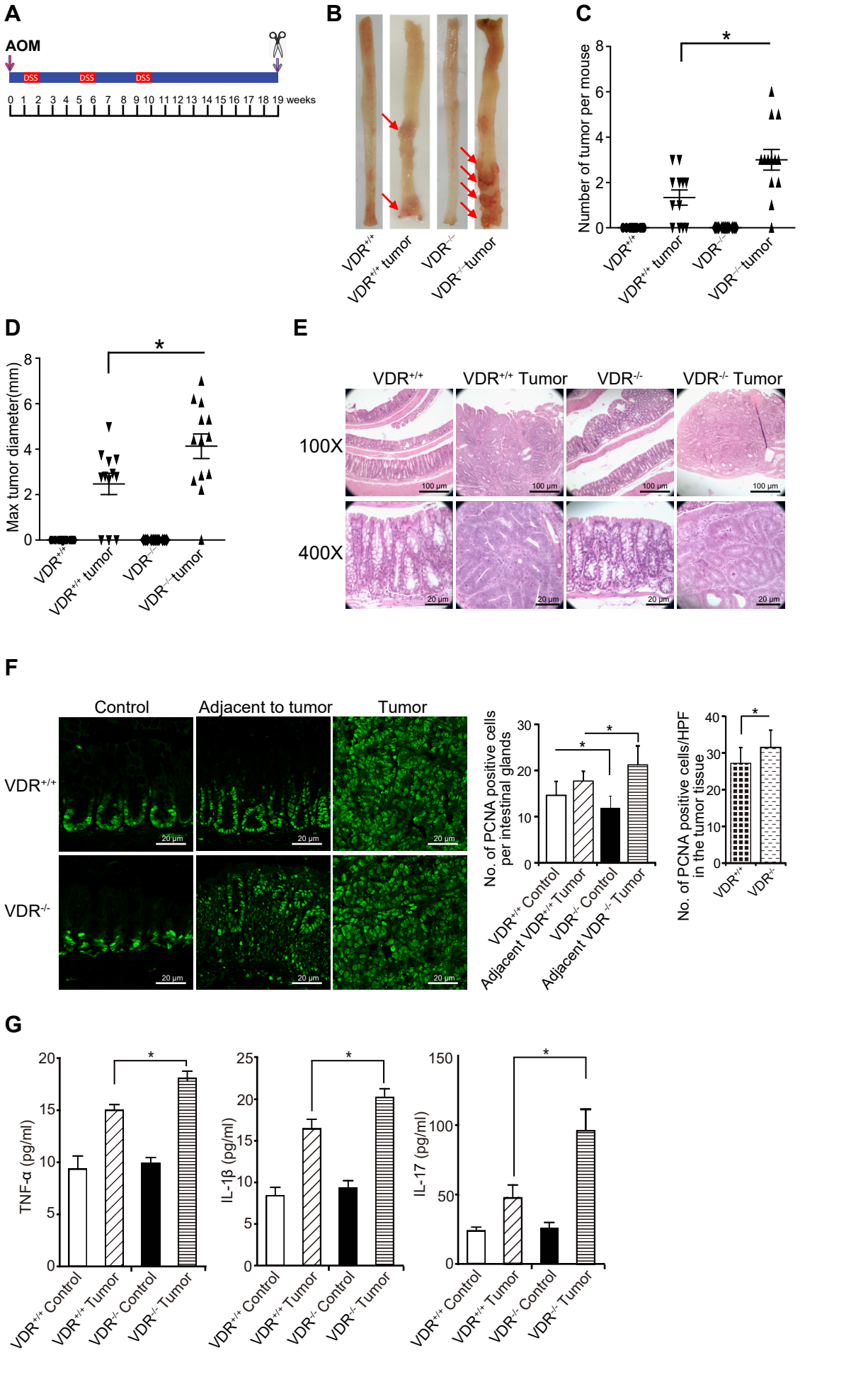

Figure. 3

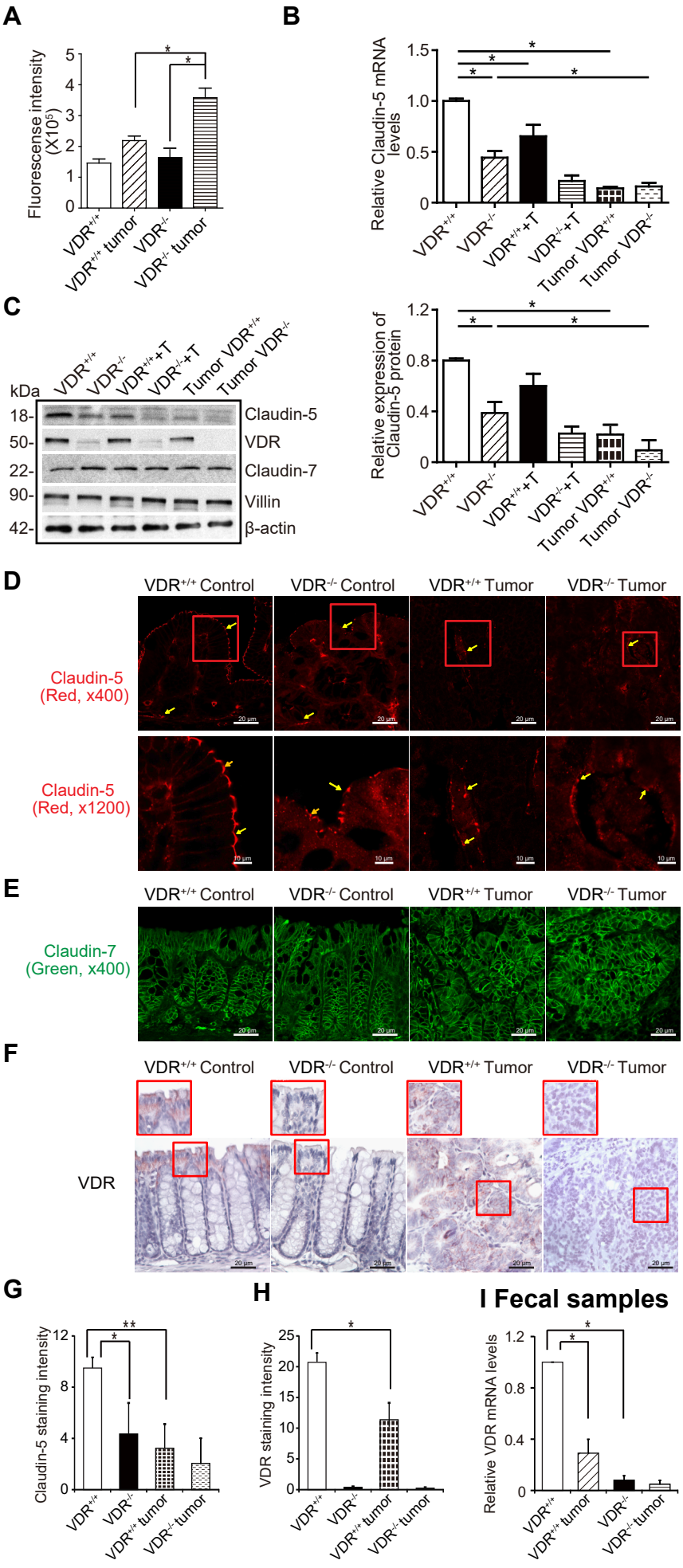

Figure. 4

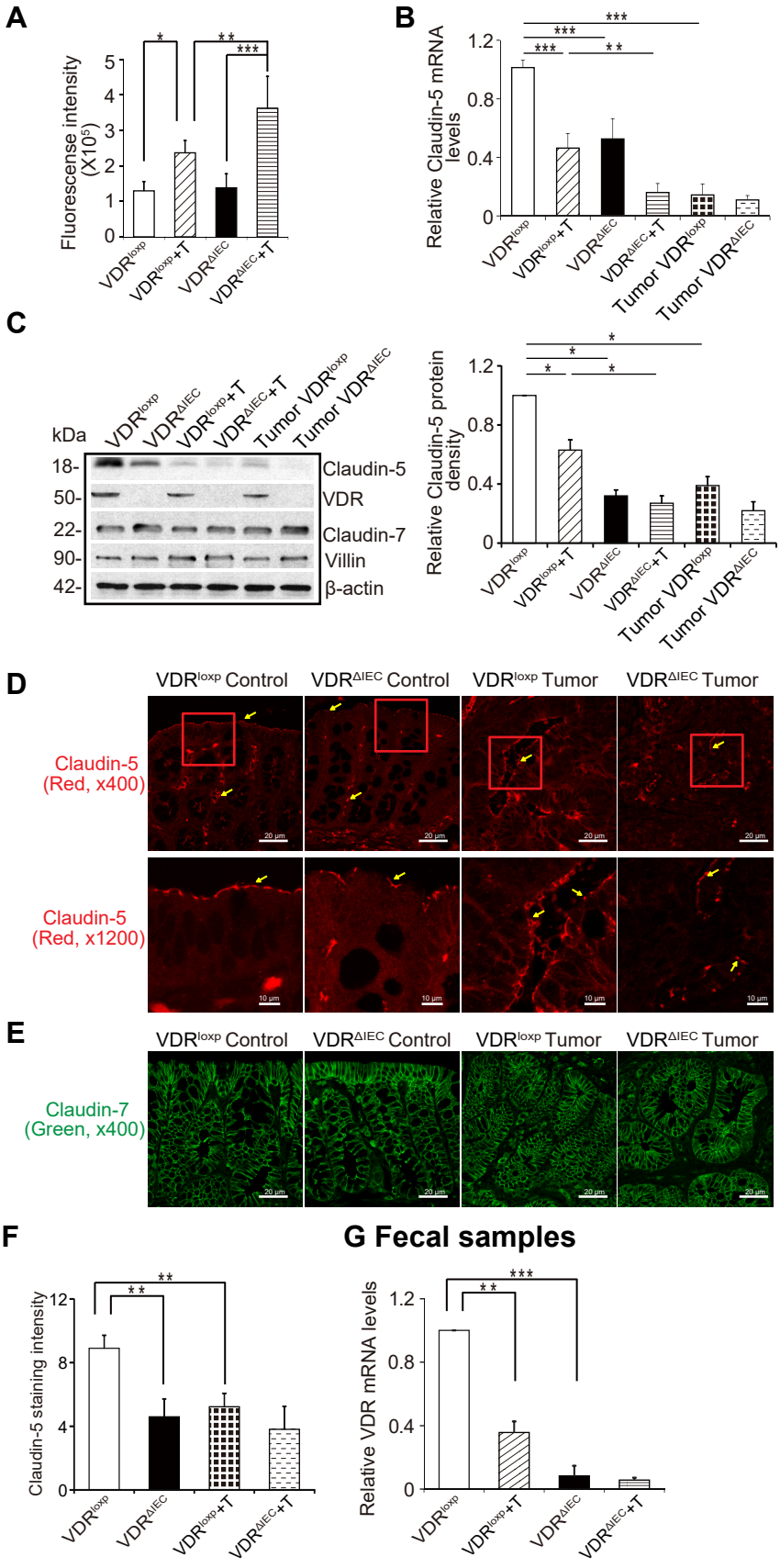

Figure. 5

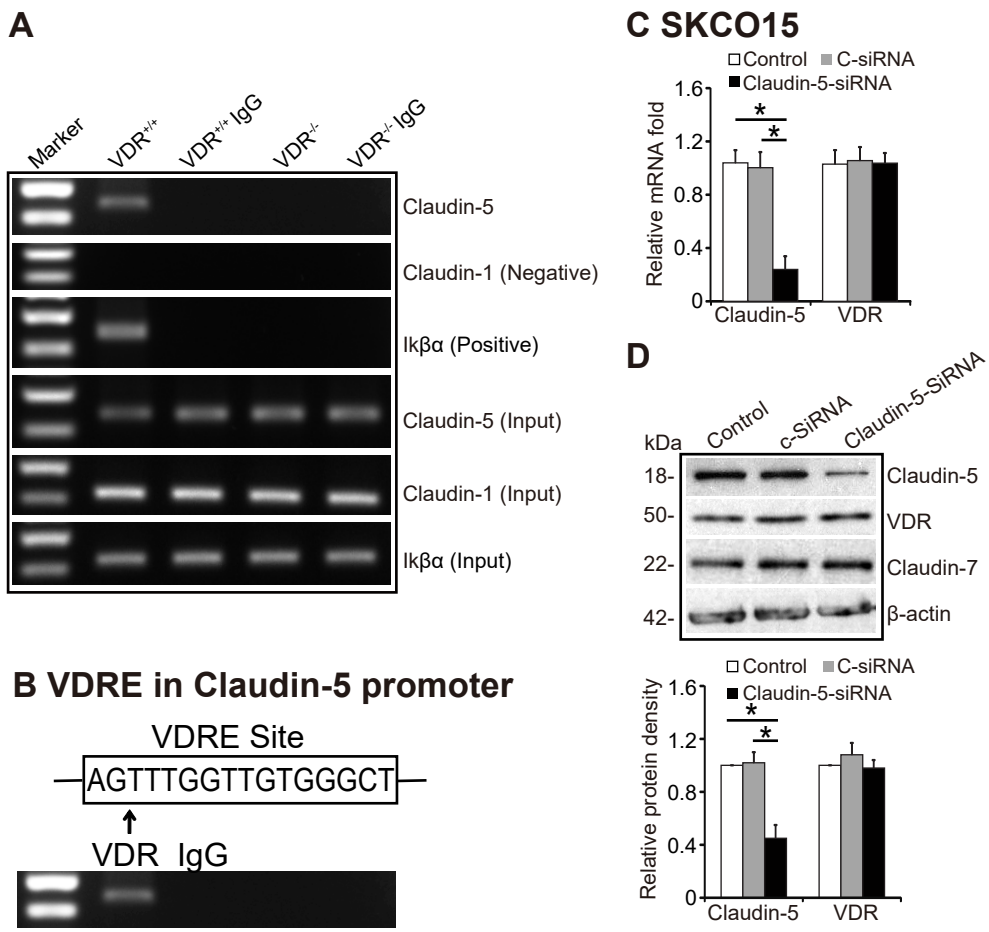

Figure. 6

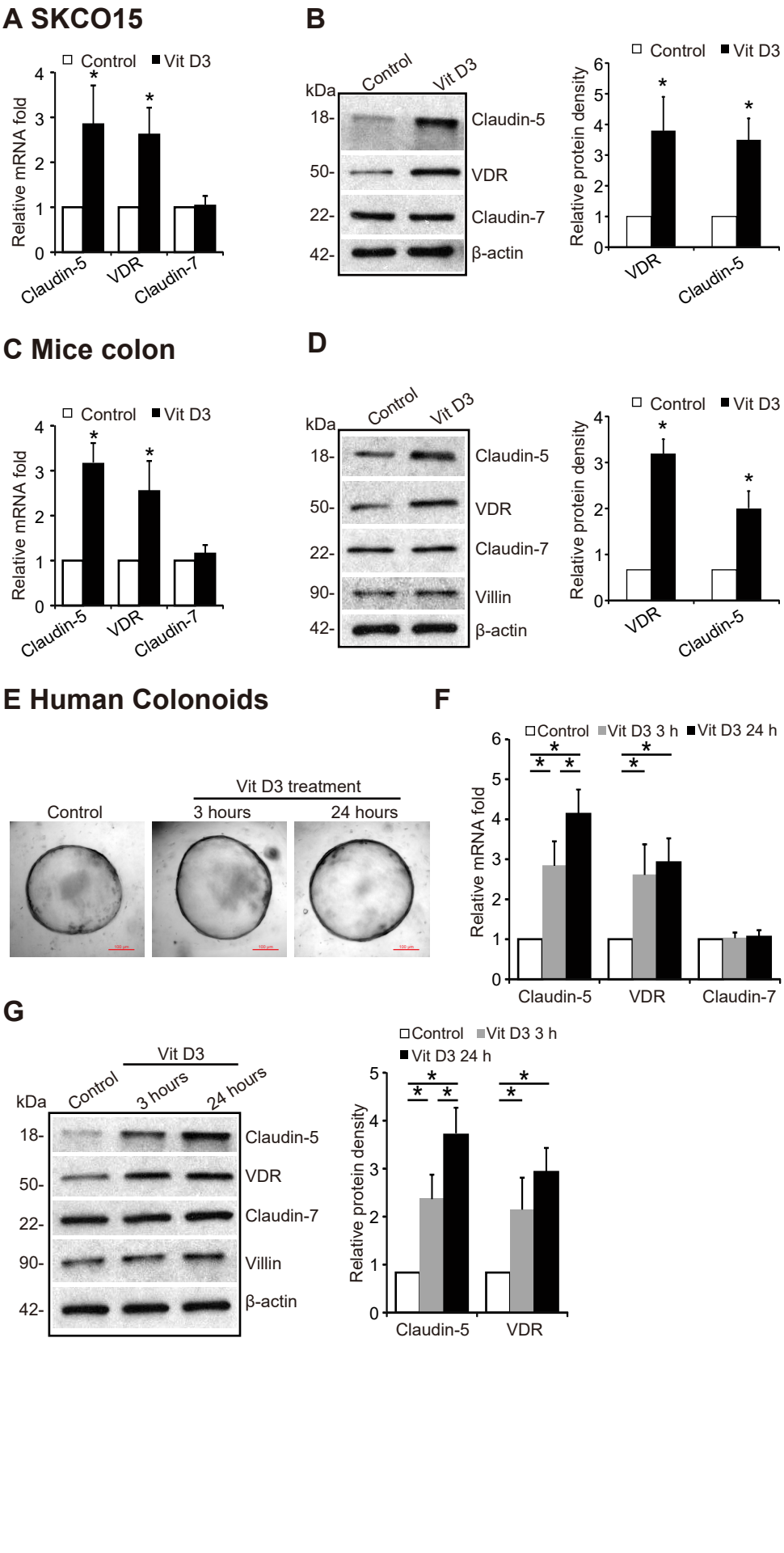

Figure. 7

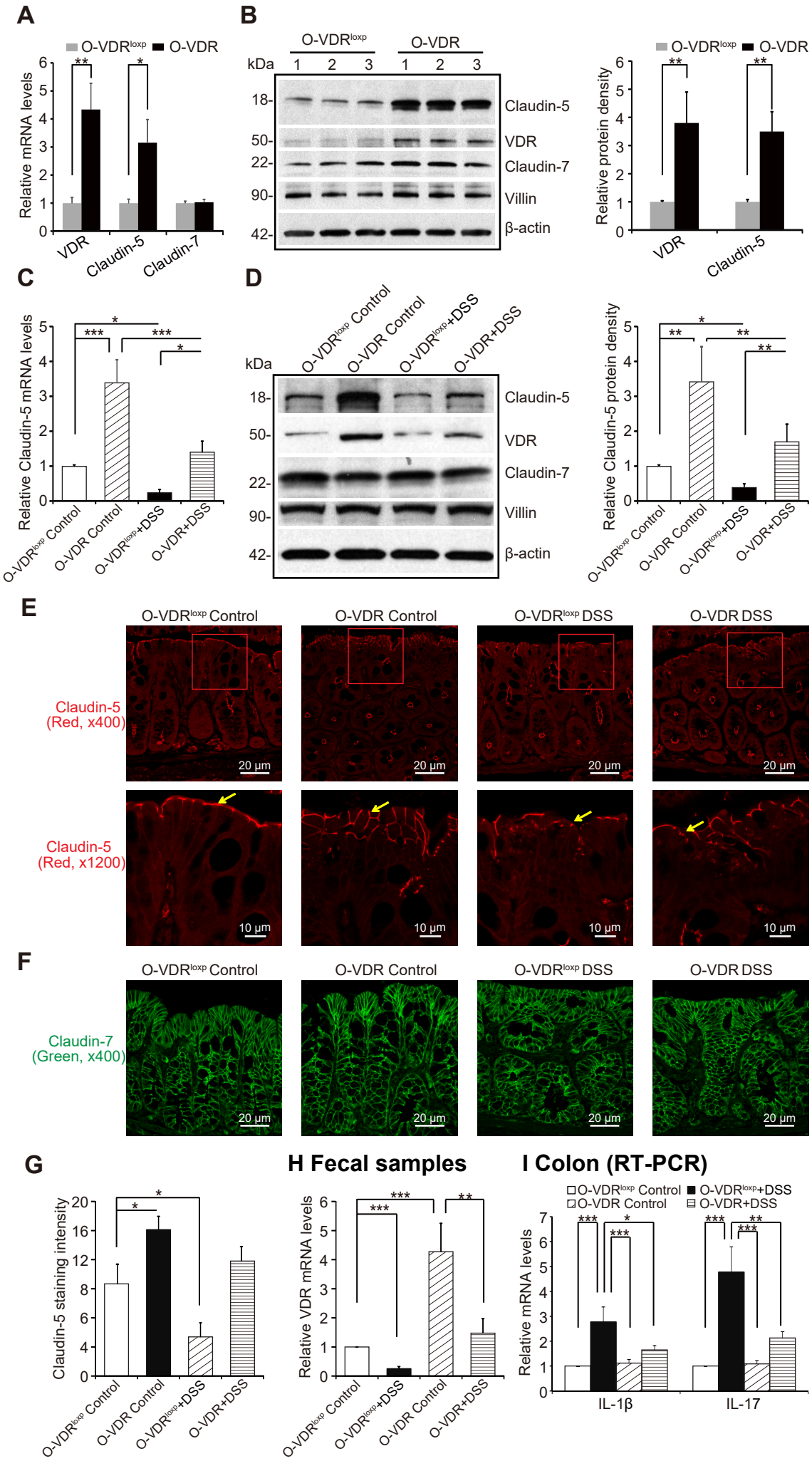

Fig. S1. VDR deficiency in intestinal epithelial cells of mice leads to the reduction of Claudin-5 at both the mRNA and protein levels *in vivo*.

(A) Claudin-5 protein and **(B)** mRNA levels were significantly lower in $VDR^{-/-}$ mice compared to levels in the $VDR^{+/+}$ mice (data are expressed as mean ± SD. n = 5, student's t-test, *P < 0.05). **(C)** Location of Claudin-5 protein in the colons of $VDR^{+/+}$ and $VDR^{-/-}$ mice. Images are from a single experiment and are representative of 5 mice per group. **(D)** Claudin-5 protein and **(E)** mRNA levels were significantly lower in $VDR^{\Delta IEC}$ mice compared to levels in the VDR^{loxp} mice (data are expressed as mean ± SD. n = 5, student's t-test, *P < 0.05). **(F)** Claudin-5 protein and **(G)** mRNA were both decreased in $VDR^{-/-}$ MEF cells (data are expressed as mean ± SD. n = 3, student's t-test, *P < 0.05). **(H)** Location and quantification of Claudin-5 protein in $VDR^{+/+}$ and $VDR^{-/-}$ MEF cells. Images are from a single experiment performed in triplicate. (Data are expressed as mean ± SD. n = 3, one-way ANOVA test, *P < 0.05).